ACS OMEGA

http://pubs.acs.org/journal/acsodf

Article

Enhancement of Both Faraday and Kerr Effects with an All-Dielectric Grating Based on a Magneto-Optical Nanocomposite Material

François Royer,* Bobin Varghese, Emilie Gamet, Sophie Neveu, Yves Jourlin, and Damien Jamon

Cite This: *ACS Omega* 2020, 5, 2886−2892

Read Online

ACCESS | Metrics & More | Article Recommendations

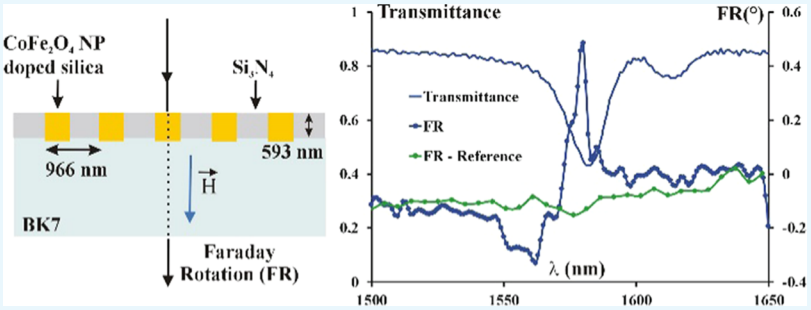

ABSTRACT: We report on the design, fabrication, and characterization of an all-dielectric one-dimensional (1D) resonant device formed by a silicon nitride grating impregnated by a low-index magneto-optical silica-type matrix. This impregnation is realized through the dipping of the 966 nm periodic template in a sol−gel solution previously doped with $CoFe_2O_4$ nanoparticles, and able to fill the grating slits. By a proper adjustment of the geometrical parameters of such a photonic crystal membrane, simultaneous excitation of transverse electric (TE) and transverse magnetic (TM) polarization resonances is nearly achieved at 1570 nm. This TE/TM phase-matching situation leads to a fivefold enhancement of the Faraday effect in the resonance area with an increased merit factor of 0.32°. Moreover, the device demonstrates its ability to enhance longitudinal and transverse Kerr effects for the other directions of the applied magnetic field. Taking benefits from the ability of the nanocomposite material to be processed on photonic platforms, and despite its quite low magneto-optical activity compared to classical magnetic materials, this work proves that an all-dielectric 1D device can produce a high magneto-optical sensitivity to every magnetic field directions.

INTRODUCTION

Magneto-optical (MO) interaction between light and a magnetized material is employed in photonics devices, which finally relates to sensing,[1−3] light modulation,[4] or optical nonreciprocity.[5,6] Depending on the orientation of the magnetization compared to that of the light plane of incidence, these devices capitalize differently on MO interaction: through the modification of the light polarization for the Faraday effect in transmission and longitudinal/polar Kerr effect in reflection (L/PMOKE), or through light intensity modification for transverse Kerr effect (TMOKE).[7] Whatever the functionality, the development of efficient MO devices usually faces two difficulties.

First, since the magnitude of MO effects is quite low, it is challenging to reduce the footprint of integrated MO devices and scale the size required to be embedded onto photonic platforms. A large area of research is thus devoted to the enhancement of MO effects, which can also be employed to increase the sensitivity of MO sensors. Several strategies have been proposed by research groups to enhance the MO effects. Currently, a large part of this activity is based on plasmonic resonances obtained in metallic materials combined with MO materials, or in ferromagnetic metals. For example, surface plasmon resonance in a one-dimensional (1D) gold grating placed on top of a magnetic film has been used to produce high enhancement of the TMOKE for transverse magnetic (TM) propagation.[8,9] Combined with transverse electric (TE) waveguide mode resonance in the garnet film, this plasmonic effect has also led to a large enhancement of the Faraday effect[10] through an energy exchange between the two modes, which boosts the MO polarization conversion. Another concept is based on extraordinary optical transmittance basically obtained in a two-dimensional (2D) metallic grating. Associated with a MO layer, these systems have mainly led to large enhancements in the Faraday rotation in the transmission mode.[11−14] Finally, when the metallic grating is placed inside the core MO layer, electromagnetic-induced absorption (EIA) phenomenon is also a way to produce a large increase in the

Received: November 4, 2019
Accepted: January 23, 2020
Published: February 4, 2020

https://dx.doi.org/10.1021/acsomega.9b03728
ACS Omega 2020, 5, 2886−2892

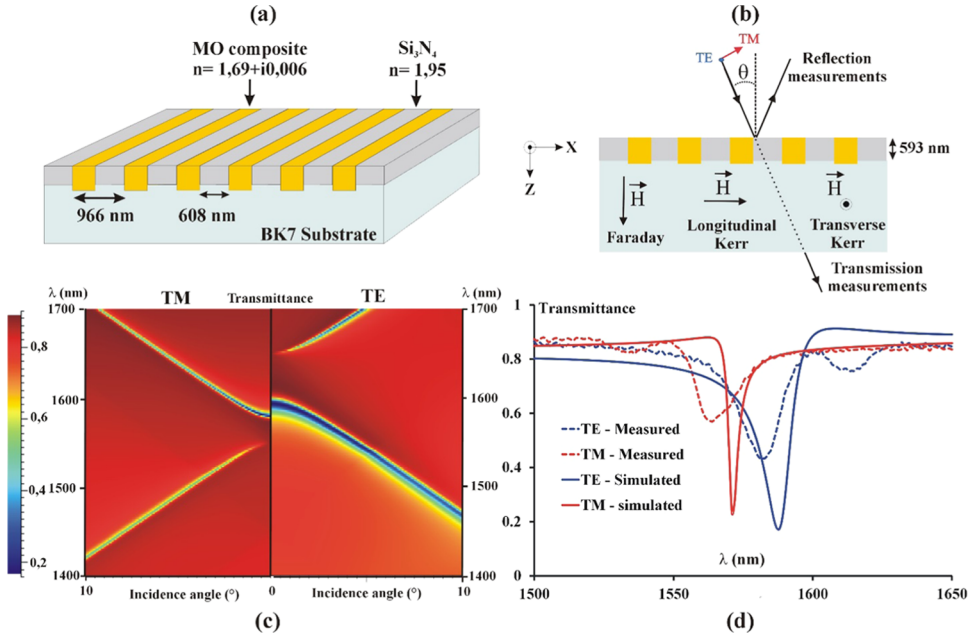

Figure 1. (a) Schematic of the device under consideration with optical/geometrical parameters. (b) Magnetic field directions used for measurements and RCWA calculations. (c) Transmittance of the device measured and calculated at normal incidence. (d) Color map of the device transmittance calculated under TM and TE polarized illuminations as a function of the wavelength and incident angle. Incident angle axis has been reversed for TM to highlight the TE/TM resonance overlap at normal incidence.

Faraday effect.[15] Apart from plasmonic effects, resonant effects based only on dielectric materials are also attractive because of their reduced intrinsic absorption, which has an impact on the quality of resonance. Thereby, resonant enhancements of the MO effects have been obtained through the sub-micrometric periodic patterning of dielectric MO materials either as 1D/2D planar structure,[16] as photonic crystals[17,18] or periodic waveguide devices.[19] MO materials can also be periodically arranged as 1D or 2D gratings with a low- or high-index material to obtain MO enhancement through waveguide-mode resonant[20] or electromagnetically induced transparency.[21] Several reviews give a large understanding of this area of research.[22−24]

However, a large part of these works relies on numerical simulations and there are few experimental demonstrations. This is due to the second limitation of the development of MO devices mentioned previously. Indeed, yttrium garnet oxides, which are the most efficient MO materials, are very challenging to process and pattern on photonic platforms[25] because of their lattice mismatch with photonic substrates and the high-temperature annealing required to be MO active.[26] Even though great progress has been made on the monolithic integration of such materials,[27] other strategies employ surface bonding onto silicon and III/V laser substrates,[26,28] or novel MO materials.[15,29,30] Thus, concerning the enhancement of the MO effects with surface devices, few experimental demonstrations that exist were largely obtained with a metallic grating placed on top of a garnet film. Belotelov and co-workers have used such devices to prove the enhancement of the Faraday effect[10] and TMOKE.[8] More recently, Floess et al. demonstrated the Faraday rotation as large as 14°, with a device thickness as low as 139 nm. Based on EIA, the device consists of a gold grating embedded in a EuS core layer at 20 K.[15] In another area of wavelength, Tamagnone et al. proved the ability of graphene metasurfaces to enhance the Faraday effect at few tetra hertz.[31] In the photonic range, experimental demonstrations of the enhancement of magneto-optical effects with an all-dielectric surface are not common, and, to the best of our knowledge, no current device has been proved to enhance different MO effects.

This work addresses these different challenges with the objective of realizing an all-dielectric 1D planar device able to enhance both the Faraday and Kerr effects at 1.5 μm. As a MO material, a nanocomposite made of $CoFe_2O_4$ nanoparticles (NPs) embedded in a silica matrix is employed because of its proven ability to be integrated on photonic platforms,[30] or processed as three-dimensional (3D) photonic crystals.[18] The objective was to associate this composite with silicon nitride as a high-refractive-index material and form a 1D photonic-crystal membrane.[32] Concerning the design, the strategy was to adjust the optogeometrical parameters of such a membrane to obtain an overlap of TE/TM photonic band edges. Thereby, TE and TM waveguide modes can be strongly coupled to each other by the MO activity of the composite material, leading to an increase of the Faraday and longitudinal Kerr effects, as they involve the conversion of orthogonal polarizations. Furthermore, the TM waveguide mode resonance can be employed to produce an enhanced TMOKE.

RESULTS AND DISCUSSION

The schematic of the device under consideration is given in Figure 1. It consists of Si_3N_4 nanostrips with a refractive index of 1.95, which alternates with a lower-index MO composite, forming a 1D periodic membrane on the BK7 substrate. The thickness of the device (593 nm) is enough to ensure the presence of waveguide modes for both polarizations (TE and TM) of around λ = 1.55 μm. The 966 nm period, Λ, is suitable to obtain a coupling of the incident light to these modes: $\beta = k_x + mK$ (1), where β is the propagation constant of a guided mode, $k_x = 2\pi \sin\theta/\lambda$ (2) is the incident wavevector, and $K = 2\pi/\Lambda$ is the grating vector. Other parameters to be fixed are the width of the Si_3N_4 strips and the refractive index of the

https://dx.doi.org/10.1021/acsomega.9b03728
ACS Omega 2020, 5, 2886−2892

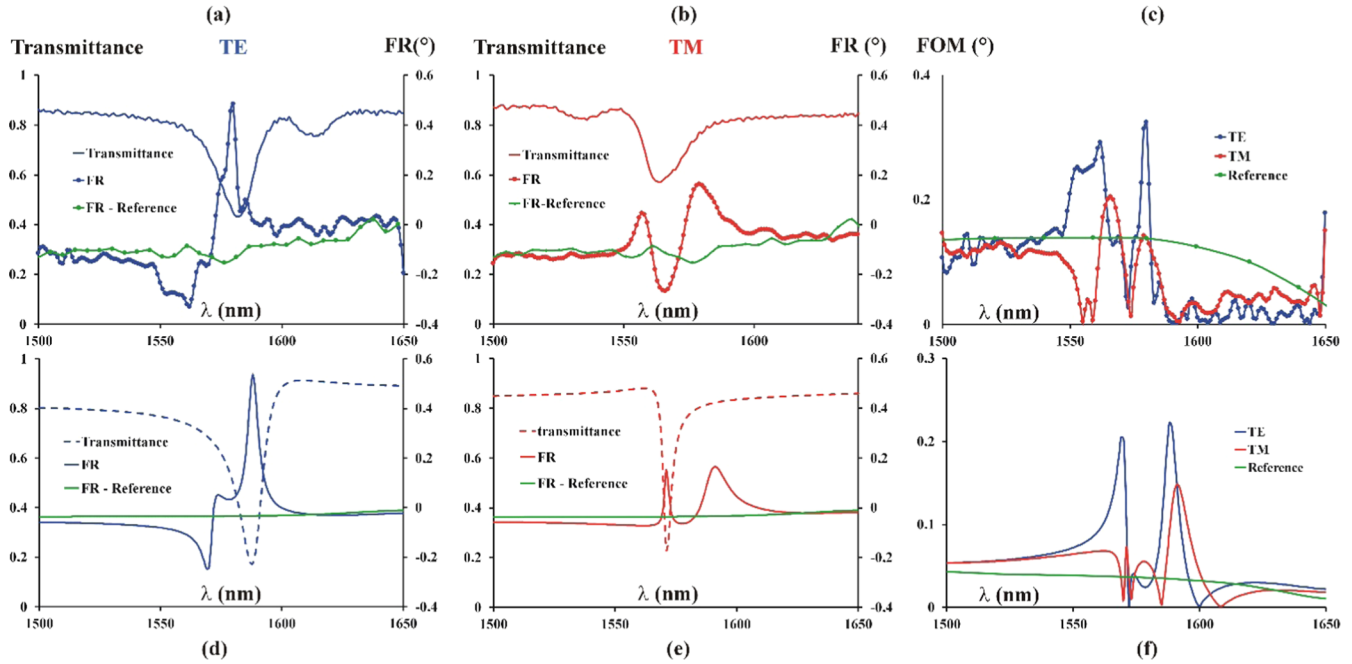

Figure 2. (a–c) Measurements. (d–f) RCWA numerical calculations. Normal incidence Faraday rotation spectrum plotted with transmittance for each polarization, and related figure of merit (FOM). The reference sample is a MO film with a thickness of 593 nm.

composite. The simultaneous excitation of TE and TM resonances at normal incidence require a proper combination of both these parameters and thickness.[33] Fine adjustment of the strip width being technologically not easy, a great advantage of the composite approach is that the refractive index of the MO material can be tuned by varying the amount of NP used to dope the initial sol–gel preparation (see Methods). Thus, from the 608 nm value of the strip width obtained after lithography processes, an optimal refractive index of 1.64 has been calculated by RCWA simulations. It corresponds to an NP volume fraction of 15% in the matrix. Based on these results, the 1D Si_3N_4 grating template has been impregnated with a sol–gel solution containing a suitable quantity of $CoFe_2O_4$ NPs previously crystallized during a co-precipitation process in water.[34] The device is finally submitted to soft thermal annealing at 100 °C, leading to a MO refractive index of 1.69 (see Methods).

Figure 1 shows both TE and TM dispersion diagrams through the 2D plot of the calculated transmittance of the device as a function of the wavelength and incident angle. As explained by Alasaarela et al.,[35] such a calculation is a straightforward way, often used by researchers, to plot the dispersion relation of waveguide grating guided modes. Indeed, due to the coupling effect of the grating (2), varying the incident wavevector angle is a way to vary the wavevector β. These plots evidence the presence of photonic band gaps for both polarizations with upper and lower bands. For a 1D photonic crystal membrane, the waveguide imposes a different dispersion relation for TE and TM with different band gap edges. However, by properly adjusting the geometrical parameters of the membrane, band edges could be made to coincide.[32] Our design strategy has led to this situation since at normal incidence the upper TM band at 1571 nm almost coincides with the lower TE band at 1588 nm. Such an overlap fits well with the enhancement of MO effects. Indeed, as explained by Belotelov et al.,[10,11] enhanced polarization conversion like the Faraday effect arises when the edge of the photonic band gaps for TE and TM polarizations coincide because the two modes can efficiently exchange energy (phase-matching condition), and the flattening of the bands at the edges reduces the light group velocity and increases the light–matter interaction.[22]

Figure 1 also compares the experimental TE and TM optical transmittances with the theoretical ones for normal incidence. One can see a good agreement between theory and measurements. Furthermore, experimental TE and TM resonances are close to each other: 1564 nm (TM) and 1582 nm (TE), i.e., a mutual separation of 18 nm. It can nevertheless be noticed that the narrowness of the theoretical dips (in TM, particularly) leads to shallower and wider dips in practice. This can be explained by the inhomogeneities of the MO gratings (surface roughness and irregularities in the impregnation and grating parameters). The spectral resolution of the spectrophotometer close to 2 nm can also explain the measured depth of the dips. The main point is the overlap between both polarization resonances, which is not fully optimal but really significant and finally constitutes the basis of MO enhancements.

Enhancement results are first reported for the Faraday effect in Figure 2 through a comparison of the experimental and calculated saturated Faraday rotation (FR) θ_F at a normal incidence for both polarizations. These MO measurements have been carried out with a homemade spectral polarimeter, which includes a calibration process useful to obtain the absolute values of both rotation and ellipticity of polarized light (see Methods). In this configuration, the magnetic field direction is perpendicular to the plane of the device (see Figure 1). The spectral area of interest, between 1450 and 1650 nm, is the most relevant for $CoFe_2O_4$ NPs because an active transition assigned to Co^{2+} ions in a tetraedric configuration produces a significant MO effect in this area.[36]

A comparison of the FR of the device with that of the reference homogeneous MO film evidences an enhancement effect that occurs due to the presence of different FR peaks

https://dx.doi.org/10.1021/acsomega.9b03728
ACS Omega 2020, 5, 2886–2892

close to the spectral positions of both polarization resonances. As expected, the close proximity of TE and TM resonances allows an efficient MO coupling between TE and TM guided-mode resonances. For TE polarization, the FR reaches two maxima: one positive (0.49°) at 1579 nm, close to TE resonance, and one negative (−0.33°) at 1562 nm, close to TM resonance, whereas FR is −0.13° for the reference thin film. In absolute terms, this rotation is multiplied by 3.5. As for the TM polarization, the resonance produces a sign inversion of FR. These curves also evidence a very good agreement between experimental and calculated values, not only regarding the spectral behavior but also the magnitude of the effects. Small differences may originate from slight deviations of technological parameters, or from the angular and spectral resolutions of the light beam employed in the MO setup (see Methods).

In spite of these enhanced rotations taking place in the resonance area, the transmittance value may be reduced at the FR resonance peak, especially for the main TE FR peak. Regardless, in the case of a sensor, it is not always required to have a high optical intensity; however, it may be the case for other applications. Thus, it is relevant to analyze the trade-off between the transmittance and the Faraday rotation through its figure of merit commonly expressed as[13]

$$\mathrm{FOM}(^\circ) = |\theta_F|.|\sqrt{T}$$

For both polarizations, the FOM off-resonance values of the device, about −0.13°, are identical to that of the reference film. For each polarization, FOM possesses different resonant peaks due to both polarization resonances. The maximum value is 0.32° for the TE incident light at 1580 nm, which is three times that of the reference. In Table 1, this value is compared to others selected in the literature and obtained with planar 1D or 2D MO devices. Concerning experimental realizations, the best value of 5.8° was obtained by Floess et al[15] with a 1D magneto-plasmonic employing a large field of 5 T and a very low temperature of measurement (20 K) required to obtain a magneto-optical activity of the EuS film. With the same kind of structure, but employing a BIG film at room temperature, Chin et al.[10] could reach a FOM of 0.48°. The value of 0.32° obtained in this work is close to the one obtained by Chen et al, but it has been obtained with a really low magneto-optical activity. Indeed, the off-diagonal element of the $CoFe_2O_4$ composite is 0.0037, whereas it is 0.016 for BIG and 0.074 for EuS (see Table 1). Concerning numerical studies mainly led on 2D MO devices, the FOM varies from 7.35° with an all-dielectric device to 0.01° with a plasmonic membrane employing cobalt. For the latter, even if the FOM is quite low, the device presents a large sensitivity to the surrounding material index, which is useful for sensors. The value of 0.32° obtained in this work is within this FOM range; however, all of these numerical studies have been led with a larger MO off-diagonal element.

Table 1. Comparison of the Figure of Merit (FOM) of Several Devices Employed to Enhance the Faraday rotation[a]

FOM (deg)	ε_{12}	MO material	device features	λ (nm)	refs
5.8 (5T)	0.074	EuS at 20 K	1D-plasmonic	750	15
0.48	0.016	BIG	1D-plasmonic	963	10
0.32	0.0037	$CoFe_2O_4$ as NP	1D-dielectric	1570	this work
∼5	0.01	*Bi-YIG*	*2D-plasmonic*	700	13
7.35	0.06	*BIG*	*2D-dielectric*	1393	21
0.75	0.01	*Bi-YIG*	*2D-plasmonic*	807	14
0.48	0.01	*Bi-YIG*	*2D-plasmonic*	963	11
0.01	0.6	*Co*	*2D-plasmonic*	710	12

[a]Three first lines relate to experimental realizations whereas the three others (italic) relate to numerical simulations only.

Finally, these comparisons evidence that even if the material employed in this work has low magneto-optical activity, the realized device could reach an interesting FOM value. It proves the potentiality of such an all-dielectric 1D membrane, presenting low absorption losses compared to the metal-based structure, to efficiently enhance the magneto-optical effects. Furthermore, with a better overlap between TE and TM resonances, the FOM should reach 0.7°.[33]

To complete this analysis of the Faraday effect of the device, the spectral behavior of the Faraday ellipticity is reported in Figure 3 in the case of a TE normal incident light. Compared to that of the reference film, which shows a slight increase in the wavelength area, the Faraday ellipticity of the device presents different resonance peaks with a sign inversion at the TE resonance position. One can also note a very good agreement between experimental and calculated curves.

Figure 3 reports the spectral behaviors of the longitudinal and transverse Kerr effects of the device. LMOKE has been carried out with a magnetic field lying in the plane of the device, and perpendicular to the grating slits, for different angles of TM incidence (from 0.8 to 2.5°). In this configuration also, optical resonances produce a large enhancement of the MO effect with a peak whose magnitude and position depend on the angle of incidence. The maximum is 0.37° at 1565 nm for an incidence angle of 1.2°. Comparing the experimental and simulated curves, one can see that the shapes are well preserved, despite a spectral shift toward low wavelengths.

The TMOKE has been measured through the difference in the intensity signal between the opposite directions of the transverse magnetic field. Due to the experimental limitations of the electromagnet in this configuration, the applied magnetic field is limited to 200 mT as opposed to 800 mT for other effects (see Methods). Nevertheless, an enhancement of the TMOKE is demonstrated in either transmission or reflection, with a mutual coherence of the corresponding experimental and simulated curves. Evidently, the TMOKE measured in the transmission is larger than that measured in reflection, as predicted by the simulation. As the TMOKE only relies on TM polarization, the overlap of TE and TM resonances is not required; however, due to the presence of a large TM optical resonance, the enhancement of the TMOKE occurs like in the case of magneto-plasmonic devices.[8]

Finally, since TMOKE is an intensity effect, whereas the effect Faraday and LMOKE are the effects of the rotation of polarization, such a device may be used as magnetic sensors to measure different components of the magnetic field with enhanced sensitivity.

To conclude, enhancements of the Faraday effect, LMOKE, and TMOKE have been experimentally demonstrated on a Si_3N_4 membrane impregnated with a magneto-optical composite made of the $CoFe_2O_4$ NPs. The results obtained in this work are mainly based on the simultaneous excitation of

https://dx.doi.org/10.1021/acsomega.9b03728
ACS Omega 2020, 5, 2886−2892

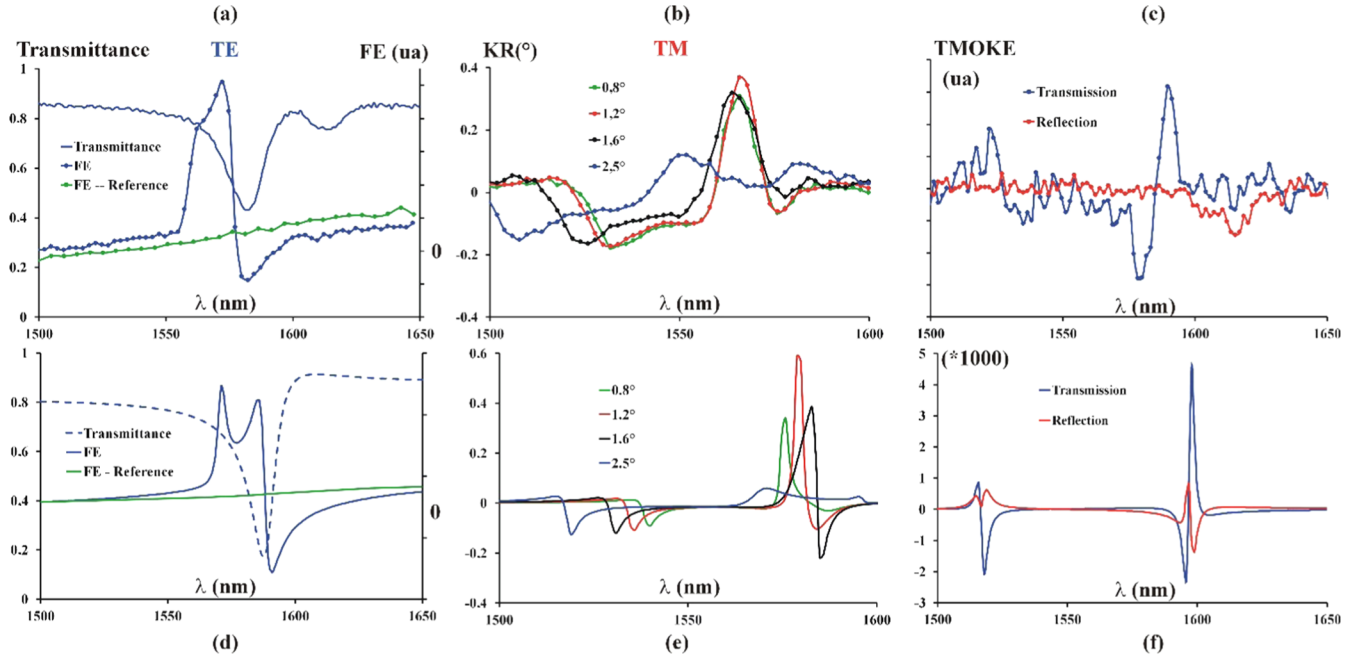

Figure 3. (a–c) Measurements. (d–f) RCWA numerical calculations. (a, d) Faraday ellipticity (FE) spectrum plotted with transmittance at the normal incidence for TE polarization. (b, e) Longitudinal Kerr rotation (KR) measured in transmittance configuration for several angles and TM polarization. (d–f) Transverse Kerr effect in transmission and reflection configurations, with TM polarization (incident angle: 2.6°).

TE and TM resonances through a proper choice of geometrical parameters of the dielectric grating. For the Faraday effect, the FOM reaches 0.32°, which is a value close to that obtained by other research groups mainly led on magneto-plasmonics devices, even if the magneto-optical activity of the composite is lower. To the best of our knowledge, this is the first time that three different magneto-optical effects have been successfully demonstrated with significant enhancement within an optical component from planar technology. In addition, these results are obtained on a single all-dielectric grating, whereas works dedicated to such enhancements in the literature commonly employed magneto-plasmonic-based devices.

METHODS

Fabrication of the Si_3N_4 grating template was subcontracted to the University of Joensuu (Finland). The first step was the deposition of a 593 nm thick silicon nitride layer on the BK-7 substrate. Then, electron beam lithography and reactive ion etching were performed to obtain the 1D template with a 966 nm period. This elaboration method ensures a very good homogeneity of the pattern over the 5 by 5 mm surface of the device. AFM investigations evidence a Si_3N_4 line width of 608 nm and a grating depth of 623 nm. Compared to the initial layer thickness, this last value indicates that the BK7 substrate has been also etched over about 30 nm. Then, the silicon nitrite refractive index was measured by ellipsometry outside the etched area. Around 1550 nm, the obtained value is 1.95, with a low dispersivity and an undetectable absorption.

Impregnation has been realized by dip-coating this template in a liquid sol–gel preparation doped by magnetic nanoparticles. This solution was obtained by the mixture of tetraethyl-orthosilicate ($Si(OC_2H_5)_4$/TEOS), chloridric acid, ethanol, and water (see ref 36 for details.). To provide a magneto-optical feature to the final silica matrix, magnetic $CoFe_2O_4$ nanoparticles dispersed as ferrofluid in water are added to the solution. The amount of NPs governs the magneto-optical activity as well as the refractive index of the final nanocomposite material.[36] After the dip-coating, thermal annealing at 100 °C is performed for 1 h. Using the optogeometrical parameters, the RCWA investigations were performed to determine the optimal refractive index value required to obtain a perfect TE/TM phase-matching condition. This optimal value is 1.64. The amount of NPs has been adjusted to reach this value, and ellipsometric measurements led to an area without Si_3N_4 grating evidenced a refractive index of 1.69 + i0.006, not exactly but not so far from the targeted value. The volume fraction of particle in the nanocomposite is thus 15%, which corresponds to an off-diagonal permittivity tensor element of ε_{MO} = 0.0015 (−2.5i + 1.2).

Optical numerical simulations were carried out using MC GRATINGS, a RCWA (Rigorous Coupled Waves Analysis)-based commercial code,[37] and the MO simulations were made with a homemade RCWA code taking into account the whole permittivity tensor.[38] The Fourier modal method (FMM) or RCWA is the most suitable numerical method to solve Maxwell's equations and analyze the interaction of electromagnetic waves with periodic diffractive structures.[39]

Transmittance measurements were carried out on a Carry5000 spectrometer with a spectral resolution of 2 nm from Agilent Technologies.

The magneto-optical behavior of the device was investigated at room temperature using a homemade polarimetric optical bench, based on a modulation technic combined with an ellipsometric-type calibration method (see ref 18 for details). This system mainly employs a xenon white light source (combined with a monochromator to select the wavelength with a spectral resolution of about 7 nm), a polarizer, a photoelastic modulator, an analyzer, a detector, and a lock-in amplifier. Such an optical arrangement is suitable to analyze the polarization state of light (rotation, ellipticity) by means of the first and second harmonic signals of the LIA.[40] The

https://dx.doi.org/10.1021/acsomega.9b03728
ACS Omega 2020, 5, 2886–2892

calibration method[41,42] allows us to measure the absolute value of the polarization rotation with a detection limit of 0.001°. The calibration coefficient, which gives the ellipticity, is not precise enough in the wavelength range to finally obtain an absolute value. During the measurement, the sample is submitted to an external magnetic field, which can vary from 0 to 0.8 T. Thus, each MO effect (Faraday or Kerr) was measured as a function of the field through a hysteresis loop curve. The saturated value is then plotted as a function of the wavelength. In terms of angular resolution, as the beam emerging from the white light source has to be focused on the sample, the incident light possesses a cone angle of the order of 3°.

AUTHOR INFORMATION

Corresponding Author

François Royer − *Université de Lyon, CNRS, UMR 5516, Institut d'Optique Graduate School, Laboratoire Hubert Curien, Université Jean-Monnet, F-42000 Saint-Etienne, France;* orcid.org/0000-0002-0632-7915; Email: Francois.Royer@univ-st-etienne.fr

Authors

Bobin Varghese − *Université de Lyon, CNRS, UMR 5516, Institut d'Optique Graduate School, Laboratoire Hubert Curien, Université Jean-Monnet, F-42000 Saint-Etienne, France*

Emilie Gamet − *Université de Lyon, CNRS, UMR 5516, Institut d'Optique Graduate School, Laboratoire Hubert Curien, Université Jean-Monnet, F-42000 Saint-Etienne, France*

Sophie Neveu − *Sorbonne Universités, UPMC Univ Paris 06, UMR 8234, PHENIX, F-75005 Paris, France*

Yves Jourlin − *Université de Lyon, CNRS, UMR 5516, Institut d'Optique Graduate School, Laboratoire Hubert Curien, Université Jean-Monnet, F-42000 Saint-Etienne, France*

Damien Jamon − *Université de Lyon, CNRS, UMR 5516, Institut d'Optique Graduate School, Laboratoire Hubert Curien, Université Jean-Monnet, F-42000 Saint-Etienne, France*

Complete contact information is available at: https://pubs.acs.org/10.1021/acsomega.9b03728

Notes

The authors declare no competing financial interest.

ACKNOWLEDGMENTS

The authors thank Joensuu University for the fabrication of the silicon nitride grating.

REFERENCES

(1) Diaz-Valencia, B. F.; Mejia-Salazar, J. R.; Oliveira, O. N., Jr; Porras-Montenegro, N.; Albella, P. Enhanced Transverse Magneto-Optical Kerr Effect in Magnetoplasmonic Crystals for the Design of Highly Sensitive Plasmonic (Bio)sensing Platforms. *ACS Omega* **2017**, *2*, 7682−7685.

(2) Ignatyeva, D. O.; Knyazev, G. A.; Kapralov, P. O.; Dietler, G.; Sekatskii, S. K.; Belotelov, V. I. Magneto-optical plasmonic heterostructure with ultranarrow resonance for sensing applications. *Sci. Rep.* **2016**, *6*, No. 28077.

(3) Caballero, B.; Garcia-Martin, A.; Cuevas, J. C. Hybrid magnetoplasmonic crsytals boost the performance of nanohole arrays as plasmonic sensors. *ACS Photonics* **2016**, *3*, 203−208.

(4) Morimoto, R.; Goto, T.; Pritchard, J.; Takagi, H.; Nakamura, Y.; Lim, P. B.; Uchida, H.; Mina, M.; Taira, T.; Inoue, M. Magnetic domains driving a Q-switched laser. *Sci. Rep.* **2016**, *6*, No. 38679.

(5) Huang, D.; Pintus, P.; Zhang, C.; Morton, P.; Shoji, Y.; Mizumoto, T.; Bowers, J. E. Dynamically reconfigurable integrated optical circulators. *Optica* **2017**, *4*, No. 23.

(6) Stadler, B. J. H.; Mizumoto, T. Integrated Magneto-Optical Materials and Isolators: A Review. *IEEE Photonics. J.* **2014**, *6*, No. 0600215.

(7) Zvezdin, A. K.; Kotov, V. A. *Modern Magnetooptics and Magnetooptical Materials*, 1st ed.; IOP Publishing: Bristol and Philadelphia; 1997.

(8) Pohl, M.; Kreilkamp, L. E.; Belotelov, V. I.; Akimov, I. A.; Kalish, A. N.; Khokhlov, N. E.; Yakovlev, D. R.; et al. Tuning of the transverse magneto-optical Kerr effect in magneto-plasmonic crystals. *New J. Phys.* **2013**, *15*, No. 075024.

(9) Halagačka, L.; Vanwolleghem, M.; Postava, K.; Dagens, B.; Pistora, J. Coupled mode enhanced giant magnetoplasmonics transverse Kerr effect. *Opt. Express* **2013**, *21*, 21741−55.

(10) Chin, J. Y.; Steinle, T.; Wehlus, T.; Dregely, D.; Weiss, T.; Belotelov, V. I.; Stritzker, B.; Giessen, H. Nonreciprocal plasmonics enables giant enhancement of thin-film Faraday rotation. *Nat. Commun.* **2013**, *4*, No. 1599.

(11) Belotelov, V. I.; Doskolovich, L. L.; Zvezdin, A. K. Extraordinary Magneto-Optical Effects and Transmission through Metal-Dielectric Plasmonic Systems. *Phys. Rev. Lett.* **2007**, *98*, No. 077401.

(12) Caballero, B.; Garcia-Martin, A.; Cuevas, J. C. Faraday effect in hybrid magneto-plasmonic photonic crystals. *Opt. Express* **2015**, *23*, 22238−22249.

(13) Khanikaev, A. B.; Baryshev, A. V.; Fedyanin, A. A.; Granovsky, A. B.; Inoue, M. Anomalous Faraday Effect of a system with extraordinary optical transmittance. *Opt. Express* **2007**, *15*, 6612−6622.

(14) Lei, C.; Tang, Z.; Wang, S.; Lia, D.; Chena, L.; Tang, S.; Du, Y. Plasmon resonance enhanced optical transmission and magneto-optical Faraday effects in nanohole arrays blocked by metal antenna. *Opt. Commun.* **2017**, *394*, 41−49.

(15) Floess, D.; Hentschel, M.; Weiss, T.; Habermeier, H.-U.; Jiao, J.; Tikhodeev, S. G.; Giessen, H. Plasmonic Analog of Electromagnetically Induced Absorption Leads to Giant Thin Film Faraday Rotation of 14°. *Phys. Rev. X* **2017**, *7*, No. 021048.

(16) Bai, B.; Tervo, J.; Turunen, J. Polarization conversion in resonant magneto-optic gratings. *New J. Phys.* **2006**, *8*, 205.

(17) Yoshimoto, T.; Goto, T.; Isogai, R.; Nakamura, Y.; Takagi, H.; Ross, C. A.; Inoue, M. Magnetophotonic crystal with cerium substituted yttrium iron garnet and enhanced Faraday rotation angle. *Opt. Express* **2016**, *24*, 8746−8753.

(18) Diwan, E. A.; Royer, F.; Jamon, D.; Kekesi, R.; Neveu, S.; Blanc-Mignon, M. F.; Rousseau, J. J. Large Spectral Modification of the Faraday Effect of 3D $SiO_2/CoFe_2O_4$ Magneto-Photonic Crystals. *J. Nanosci. Nanotechnol.* **2016**, *16*, 10160−10165.

(19) Dissanayake, N.; Levy, M.; Chakravarty, A.; Heiden, P. A.; Chen, N.; Fratello, V. J. Magneto-photonic crystal optical sensors with sensitive covers. *Appl. Phys. Lett.* **2011**, *99*, No. 091112.

(20) Maksymov, I. S.; Hutomo, J.; Kostylev, M. Transverse magneto-optical Kerr effect in subwavelength dielectric gratings. *Opt. Express* **2014**, *22*, 8720−5.

(21) Christofi, A.; Kawaguchi, Y.; Alu, A.; Khanikaev, A. B. Giant enhancement of Faraday rotation due to electromagnetically induced transparency in all-dielectric magneto-optical metasurfaces. *Opt. Lett.* **2018**, *43*, 1838−1841.

(22) *Magnetophotonics: From Theory to Applications*, Inoue, M.; Inoue, M.; Levy, M.; Baryshev, A. V., Eds.; Springer Series in Materials; Springer, 2013; pp 178.

(23) Maksymov, I. S. Magneto-Plasmonics and Resonant Interaction of Light with Dynamic Magnetisation in Metallic and All-Magneto-Dielectric Nanostructures. Review. *Nanomaterials* **2015**, *5*, 577−613.

(24) Armelles, G.; Cebollada, A.; García-Martín, A.; Ujué González, M. Magnetoplasmonics: Combining Magnetic and Plasmonic Functionalities. *Adv. Opt. Mater.* **2013**, *1*, 10−35.

(25) Onbasli, M. C.; Beran, L.; Zahradník, M.; Kucera, M.; Antoš, R.; Mistrík, J.; Dionne, G. F.; Veis, M.; Ross, C. A. Optical and magneto-optical behavior of Cerium Yttrium Iron Garnet thin films at wavelengths of 200−1770 nm. *Sci. Rep.* **2016**, *6*, 23640.
(26) Huang, D.; Pintus, P.; Bowers, J. E. Towards heterogeneous integration of optical isolators and circulators with lasers on silicon. *Opt. Mater. Express* **2018**, *8*, 2471−2483.
(27) Sun, X. Y.; Du, Q.; Goto, T.; Onbasli, M. C.; Kim, D. H.; Aimon, N. M.; Hu, J.; Ross, C. A. Single-Step Deposition of Cerium-Substituted Yttrium Iron Garnet for Monolithic On-Chip Optical Isolation. *ACS Photonics* **2015**, *2*, 856−863.
(28) Mizumoto, T.; Baets, R.; Bowers, J. E. optical nonreciprocal devices for silicon photonics using wafer-banded magneto-optical garnet devices. *MRS Bull.* **2018**, *43*, 419−424.
(29) Shimizu, H.; Zayets, V. Plasmonic isolator for photonic integrated circuits. *MRS Bulletin* **2018**, *43*, 425−429.
(30) Amata, H.; Royer, F.; Choueikani, F.; Jamon, D.; Parsy, F.; Broquin, J. E.; Neveu, S.; Rousseau, J. J. Hybrid magneto-optical mode converter made with a magnetic nanoparticles-doped SiO2/ZrO_2 layer coated on an ion-exchanged glass waveguide. *Appl. Phys. Lett.* **2011**, *99*, No. 251108.
(31) Tamagnone, M.; Slipchenko, T. M.; Moldovan, C.; Liu, P. Q.; Centeno, A.; Hasani, H.; Zurutuza, A.; Ionescu, A. M.; Martin-Moreno, L.; Faist, J.; Mosig, J. R.; Kuzmenko, A. B.; Poumirol, J. M. Magnetoplasmonic enhancement of Faraday rotation in patterned graphene metasurfaces. *Phys. Rev. B* **2018**, *97*, No. 241410.
(32) Gerace, D.; Andreani, L. C. Gap maps and intrinsic diffraction losses in one-dimensional photonic crystal slabs. *Phys. Rev. E* **2004**, *69*, No. 056603.
(33) Gamet, E.; Varghese, B.; Verrier, I.; Royer, F. Enhancement of magneto-optical effects by a single 1D all dielectric resonant grating. *J. Phys. D: Appl. Phys.* **2017**, *50*, No. 495105.
(34) Kekesi, R.; Royer, F.; Jamon, D.; Blanc Mignon, M.-F.; Abou-Diwan, E.; Chatelon, J. P.; Neveu, S.; Tombacz, E. 3D magneto-photonic crystal made with cobalt ferrite nanoparticles silica composite structured as inverse opal. *Opt. Mater. Express* **2013**, *3*, 935−947.
(35) Alasaarela, T.; Zheng, D.; Huang, L.; Priimagi, A.; Bai, B.; Tervonen, A.; Honkanen, S.; Kuittinen, M.; Turunen, J. Single-layer one-dimensional nonpolarizing guided-mode resonance filters under normal incidence. *Opt. Lett.* **2011**, *36*, 2411−3.
(36) Fontijn, W. F. J.; Van Der Saag, P. J.; Feiner, L. F.; Metselaar, R.; Devillers, M. A. C. A consistent interpretation of the magneto-optical spectra of spinel type ferrites. *J. Appl. Phys.* **1999**, *85*, 5100−5105.
(37) Lyndin, N. *MC Grating Software*, www.mcgrating.com.
(38) Li, L. Reformulation of the fourier modal method for surface-relief gratings made with anisotropic materials. *J. Mod. Opt.* **1998**, *45*, 1313−34.
(39) Doskolovich, L. L.; Soifer, V. A. Modelling of Periodic Diffractive Micro-and Nanostructures, In *Diffractive Nanophotonics*, Soifer, V. A., Ed.; CRC Press: Bota Raton, 2014; pp 1994−239.
(40) Drevillon, B. Phase modulated ellipsometry from the ultraviolet to the infrared: in-situ application to the growth of semiconductors. *Prog. Cryst. Growth Charact. Mater.* **1993**, *27*, 1−87.
(41) Jellison Jr, G. F. A.; Modine, F. Accurate calibration of a photo-elastic modulator in polarization modulation ellipsometry. *Proc. SPIE* **1990**, *1166*, 231.
(42) Kouko, S. L.; Llinares, C. Calibration of two different types of modulators for an application in spectroscopic phase modulated ellipsometry. *J. Phys. III* **1995**, *5*, 1211−1227.

https://dx.doi.org/10.1021/acsomega.9b03728
ACS Omega 2020, 5, 2886−2892